Supporting Information: Techno-economic analysis of large scale production of poly(oxymethylene) dimethyl ether fuels from methanol in water-tolerant processes

Yannic Tönges[a], Vincent Dieterich[b], Sebastian Fendt[b], Hartmut Spliethoff[b], Jakob Burger*[a]

[a] *Technical University of Munich, Campus Straubing for Biotechnology and Sustainability, Laboratory of Chemical Process Engineering, Uferstraße 53, Straubing, 94315, Bavaria, Germany.*
[b] *Technical University of Munich, TUM School of Engineering and Design, Chair of Energy Systems, Boltzmannstraße 15, Garching, 85748, Bavaria, Germany.*
**Corresponding author: burger@tum.de*

1. Additional information on the processes

This section gives process flow diagrams, stream tables, energy balances, and descriptions of the investigated processes. For processes for which the full stream and energy tables were not available in the original literature but calculated in this work, the specifications used as input for the simulation are highlighted in **bold**.

1.1. Process I: Production of FA with complete conversion of ME

Process I produces an aqueous solution of 0.5 g/g FA. We chose the BASF silver process, which uses a reactor with a silver catalyst and complete conversion of ME in one pass [1]. The left panel in Figure 1 shows the respective process flow diagram (PFD). The reactor conversion and selectivity as well as the composition of the Feed, the absorber off-gas, and the absorber bottom product are adopted from Ullmann's Encyclopedia of Industrial Chemistry [1].

Methanol (1) is evaporated in the evaporator E1 and mixed with steam, air (2), and recycled off-gas (9) from the absorber A1, mainly composed of N_2 and H_2. The recycle mass flow rate is adjusted so that the resulting mixture is outside of the explosive limits. The explosive limits are calculated considering the limiting oxygen concentration of the mixture [2, 3]. The gaseous mixture (3) is superheated in heat exchanger HX1 and passed over a shallow bed of silver crystals. The water in the mixture enhances conversion and selectivity; the optimal molar ratio of ME to Water is **60/40** [4]. The product leaves the reactor at **680** °C, conversion of ME is **99%**, the yield **90%** [1]. The reactor product (4) is immediately cooled in HX2 to prevent the disintegration of gaseous FA; the excess heat is utilized to produce steam.
The cooled gases (5) are fed to the bottom of the absorption column A1, modeled with **4** vapor-liquid equilibrium (VLE) stages. At the bottom of A1, a liquid solution is drawn, cooled, and recycled to its top. Water is added to the top of A1 to enhance FA absorption. The off-gases (7) from the

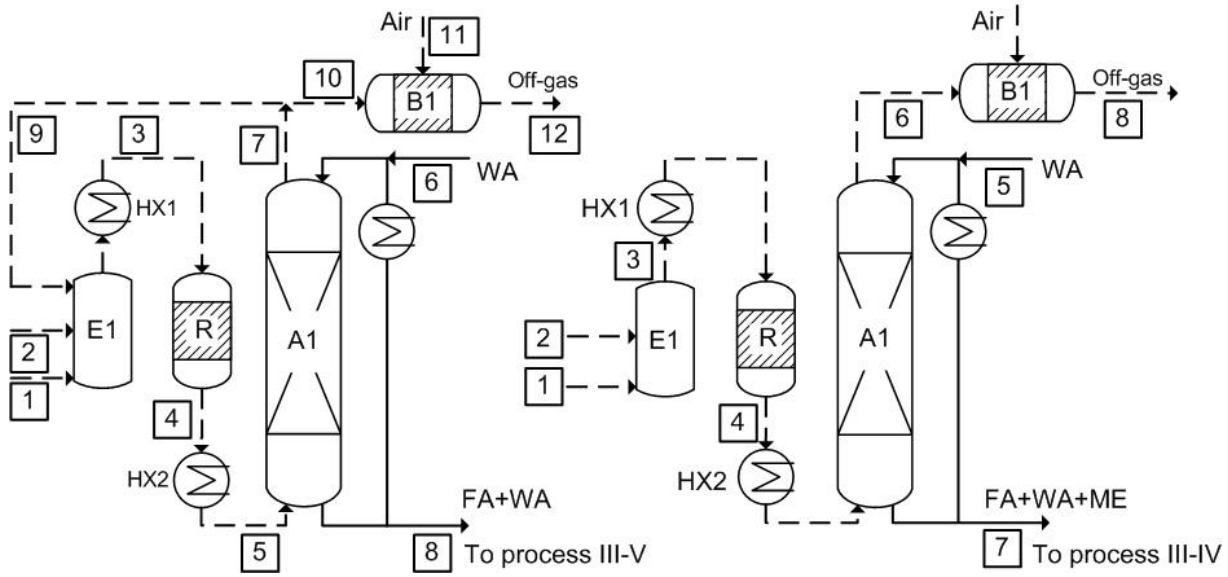

Figure 1: Process flow diagram of Process I (left panel) and Process II (right panel).

absorber contain small traces of FA and ME. Part of them are recycled as stream (9), the remainder is burned in the burner B1 with excess air (11) to generate steam. The solution (8) drawn from the bottom of A1 contains 0.5 g/g FA and WA with small traces of ME. Tables 1 and 2 give the stream table and unit data of the process.

Table 1: Stream Table Process I

Stream	1	2	3	4	5	6	7	8	9	10	11	12
$\dot{m}$ / kg/h	942.57	1354.52	4091.58	4091.59	4091.59	136.90	2991.55	1236.93	1794.50	1197.05	565.98	1763.03
p / bar	1.00	1.00	**1.00**	1.00	1.00	1.00	**1.00**	1.00	1.00	1.00	1.00	1.00
T/°C	25.00	25.00	241.97	**679.18**	160.00	25.00	**35.51**	65.61	35.51	35.51	25.00	160.00
x_i / g/g												
FA	-	-	-	**0.153**	0.153	-	**0.001**	**0.504**	0.001	0.001	-	-
WA	0.216	-	**0.068**	**0.146**	0.146	1.000	0.042	0.492	0.042	0.042	-	0.105
ME	0.784	-	**0.181**	**0.002**	0.002	-	0.001	0.003	0.001	0.001	-	-
CO_2	-	-	0.031	0.053	0.053	-	0.072	-	0.072	0.072	-	0.054
N_2	-	0.767	0.634	0.634	0.634	-	0.868	-	0.868	0.868	0.767	0.835
O_2	-	0.233	0.078	0.001	0.001	-	0.002	-	0.002	0.002	0.233	0.007
H_2	-	-	0.005	0.009	0.009	-	0.012	-	0.012	0.012	-	-
CO	-	-	0.001	0.002	0.002	-	0.003	-	0.003	0.003	-	-

Table 2: Unit operations data Process I

Unit:	T/°C	p / bar	$\dot{Q}$ / kW
E_1	49.04	1.00	405.03
HX_{1_1}	140.00	1.00	129.11
HX_{1_2}	210.00	1.00	103.18
HX_{1_3}	241.97	1.00	46.68
R	680.00	1.00	-
HX_{2_1}	300.00	1.00	-643.71
HX_{2_2}	230.00	1.00	-110.37
HX_{2_3}	160.00	1.00	-107.84
A_1	35.51	1.00	-394.29
B_{1_1}	300.00	1.00	-365.15
B_{1_2}	230.00	1.00	-39.65
B_{1_3}	160.00	1.00	-39.10

1.1.1. Process II: Production of FA with incomplete conversion of ME

The production of FA with incomplete conversion of methanol is similar to Process I. The right panel in Figure 1 shows the respective PFD. Besides FA and WA, the reactor product (4) also contains unreacted ME. It is absorbed in water, resulting in liquid (7). The absorber off-gas (6) is burned with air to generate steam; a recycle is not required. An advantage is the reactor's lower conversions, which could lead to higher selectivities. We adopted the operating point of the reactor and the resulting absorber product from the literature; it consists of 0.509 g/g FA, 0.205 g/g ME, and Water [5]. Tables 3 and 4 give the stream table and unit data of the process.

Table 3: Stream Table Route 4 Process II

Stream	1	2	3	4	5	6	7	8
$\dot{m}$ / kg/h	1125.20	1270.35	2395.55	2395.55	174.47	1345.57	1224.48	3002.25
p / bar	1.00	1.00	1.00	**1.00**	2.75	1.00	**1.00**	1.00
T/°C	25.00	25.00	44.90	705.74	25.00	25.03	**69.50**	160.00
x_i / g/g								
FA	-	-	-	**0.264**	-	0.008	**0.509**	-
WA	-	-	-	**0.092**	0.876	0.016	**0.286**	0.144
ME	1.000	-	0.470	**0.106**	0.124	0.018	0.205	0.000
CO_2	-	-	-	**0.112**	-	0.199	-	0.105
N_2	-	0.770	0.408	**0.408**	-	0.727	-	0.751
O_2	-	0.230	0.122	**-**	-	-	-	-
H_2	-	-	-	0.018	-	0.032	-	-
CO	-	-	-	-	-	-	-	-

Table 4: Unit operations data Route 4 Process II

Unit:	T/°C	p / bar	$\dot{Q}$ / kW
E_1	44.90	1.00	381.19
HX_{1_1}	140.00	1.00	79.56
HX_{1_2}	210.00	1.00	63.37
R	705.74	1.00	-
HX_{2_1}	300.00	1.00	-480.84
HX_{2_2}	230.00	1.00	-74.41
HX_{2_3}	160.00	1.00	-71.65
B_{1_1}	300.00	1.00	-1321.30
B_{1_2}	230.00	1.00	-69.86
B_{1_3}	160.00	1.00	-68.70
A_1	25.00	1.00	-644.68

1.1.2. Process II': Production of FA and fast condensation

A process proposed by Kloepper et al. [6] suggests the fast condensation of the reactor product of an FA plant with incomplete conversion. Figure 2 gives a PFD of the process. All stream compositions are adopted from the original work.

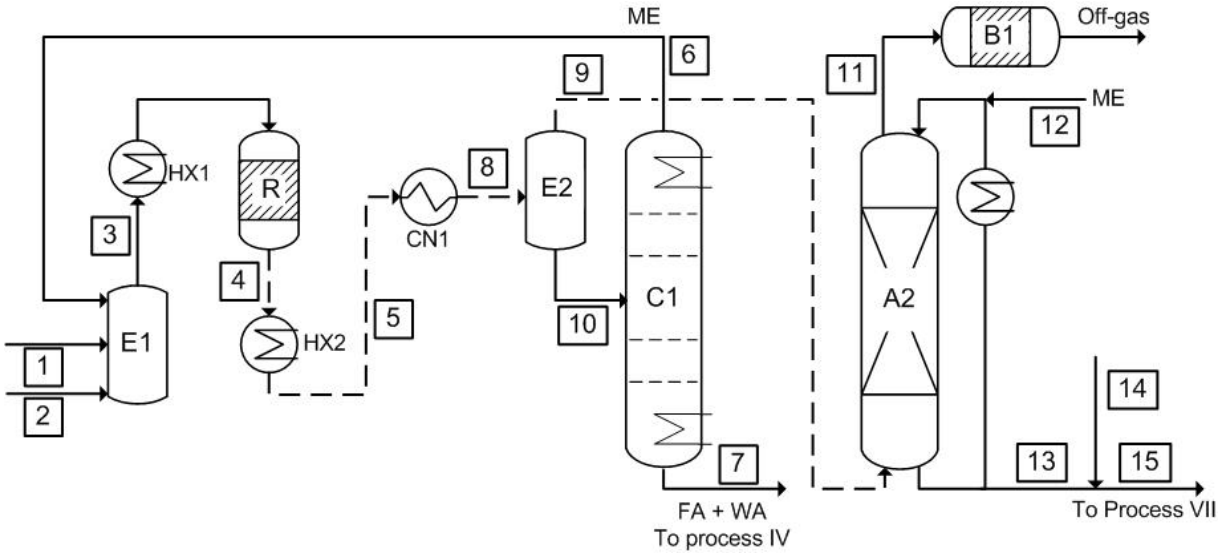

Figure 2: PFD of the process proposed by Kloepper et al..

The reactor product (4) (neglecting noncondensable components) consists of **0.445** g/g FA and **0.314** g/g ME and Water. It is subsequently cooled in HX1 to prevent the disintegration of FA. The obtained stream (5) is fed to condenser CN1. CN1 rapidly cools stream (5) to **53**°C, and the phase separator E2 splits it into the water-rich liquid (10) and the FA-rich gaseous stream (9). Stream (9) is absorbed in ME in the absorber A2 that has recirculation. The product (13) consists of 0.628

g/g FA, 0.311 g/g ME, and WA.
Stream (10) is fed to distillation column C1, where pure ME is recovered at the top (6) and recycled, and aqueous FA solution is removed as the bottom product (7). Depending on demand, product (7) can be sold as aqueous FA solution. Here stream (7) is also converted to OME feedstock using a pervaporation unit (Process VI), allowing a better comparison to the other routes. Tables 5 and 6 give the stream table and unit data of process II', tables 19 and 20 of the added pervaporation process (cf. Section 1.1.5). The mixed end product fed to process VII are 1030.61 kg of a solution of 0.603 g/g FA, 0.367 g/g ME and 0.03 g/g WA.

Table 5: Stream Table Process II'

Stream	1	2	3	4	5	6	7	8	9	10	11	12	13	14	15
$\dot{m}$ / kg/h	1438.22	1174.79	2613.00	2613.00	2613.00	335.30	670.94	2613.00	1605.87	1007.13	1220.60	33.30	418.56	29.70	448.27
p / bar	1.00	1.00	1.00	1.00	1.00	1.00	1.00	1.03	1.03	1.03	1.03	1.03	1.03	1.03	1.03
T/°C	25.00	25.00	43.89	810.12	160.00	64.57	99.20	**53.00**	**53.00**	**53.00**	11.18	16.00	23.99	25.00	26.22
x_i / g/g															
FA	-	-	-	**0.242**	0.242	-	0.542	0.242	**0.167**	**0.361**	**0.004**	-	0.629	-	0.587
WA	-	-	-	**0.131**	0.131	0.014	0.451	0.131	**0.022**	**0.305**	0.007	-	0.059	-	0.055
ME	-	1.000	**0.450**	**0.171**	0.171	**0.985**	**0.007**	0.171	0.069	0.333	**0.011**	**1.000**	0.311	1.000	0.357
CO_2	-	-	-	0.028	0.028	-	-	0.028	0.046	-	0.060	-	-	-	-
N_2	0.770	-	0.424	0.424	0.424	-	-	0.424	0.689	-	0.907	-	-	-	-
O_2	0.230	-	**0.127**	-	-	-	-	-	-	-	-	-	-	-	-
H_2	-	-	-	0.004	0.004	-	-	0.004	0.007	-	0.009	-	-	-	-
CO	-	-	-	-	-	-	-	-	-	-	-	-	-	-	-

Table 6: Unit operations data Process II'

Unit:	T/°C	p / bar	$\dot{Q}$ / kW
E_1	43.89	1.00	397.13
HX_{1_1}	140.00	1.00	86.82
CN_1	53.00	1.03	-629.44
R	810.12	1.00	-
HX_{2_1}	300.00	1.00	-643.70
HX_{2_2}	230.00	1.00	-76.11
HX_{2_3}	160.00	1.00	-72.77
B_{1_1}	300.00	1.00	-313.15
B_{1_2}	230.00	1.00	-39.13
B_{1_3}	160.00	1.00	-38.61

Distillation columns	C_1
$\dot{Q}_{top}$ / kW	-549.87
T_{top}/°C	64.57
$\dot{Q}_{bot}$ / kW	605.37
T_{bot}/°C	99.20
p / bar	1.00
N	24.00
N^{Feed}	10.00
RR	4.28

1.1.3. Process III: Thin-film evaporation

The technology to produce stable, highly concentrated FA solutions using thin-film evaporators (TFE) is well established [7, 8, 9]. In previous work [10], we developed a process that employs a TFE to produce OME-feedstock from either aqueous FA (Route 1) or water-methanol formaldehyde solutions (Route 4), Figure 3 shows a PFD. The process is adopted without modification; complete stream tables and energy balances are taken from the original literature [10].

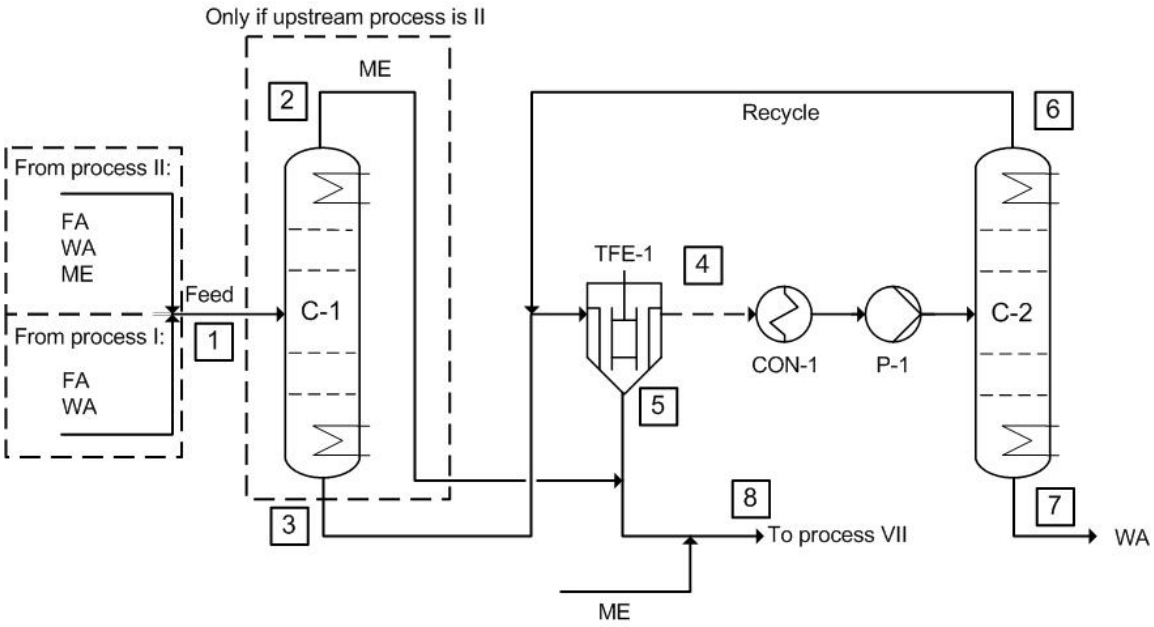

Figure 3: PFD of Process III. C1 is only required if the Feed contains methanol (Route 4)

The feed (1) is fed to distillation column C1, where parts of the methanol are removed as the top product (2) (Column C1 is not required in Route 1, and the feed is fed directly to the thin-film evaporator TFE1). The bottom product (3) is fed to the thin-film evaporator TFE1, in which it is partially evaporated, yielding a gaseous, FA-lean top product (4). The liquid residual (5) of the TFE is a concentrated FA solution with small amounts of ME and WA. It is mixed with ME to yield the OME feedstock (8). The top product (4) of TFE1 is condensed in the condenser CON1 and fed to the distillation column C2. C2 removes pure WA as the bottom product (7), the top product (6) is recycled, mixed with stream (3), and fed to TFE1. Based on the fed FA solution, the OME-feedstock contains 0.1 (Route 1) or 0.12 (Route 4) g/g water. Tables 7 to 9 give the stream table and unit data of the process for Route 1, tables 10 to 12 for Route 4.

Table 7: Stream Table Process III, Route 1

Stream	1	4	5	6	7	8
$\dot{m}$ / kg/h	1236.93	806.10	762.40	331.56	474.54	1135.98
p / bar	25.00	0.20	0.20	4.00	4.00	1.00
T/°C	65.61	120.47	120.47	136.19	143.47	100.73
x_i / g/g						
FA	0.504	0.222	0.816	0.536	0.003	0.548
WA	0.492	0.772	0.178	0.449	0.997	0.120
ME	0.003	0.006	0.005	0.015	-	0.332

Table 8: Unit operations data Process III, Route 1

Unit:	T/°C	p / bar	$\dot{W}$ / kW	$\dot{Q}$ / kW
TFE	120.47	0.20	-	528.16
CON_1	45.00	0.20	-	-535.84

Table 9: Columns Process III, Route 1

Distillation columns	C_2
$\dot{Q}_{top}$ / kW	-439.44
T_{top}/°C	136.19
$\dot{Q}_{bot}$ / kW	544.88
T_{bot}/°C	143.47
p / bar	4.00
N	24.00
N^{Feed}	14.00
RR	1.73

Table 10: Stream Table Process III, Route 4

Stream	1	2	3	4	5	6	7	8
$\dot{m}$ / kg/h	1224.48	212.85	1011.63	619.15	771.79	379.31	239.84	1111.10
p / bar	1.00	0.50	0.50	0.20	0.20	4.00	4.00	40.00
T/°C	69.50	47.84	83.43	118.12	118.12	135.22	143.67	105.42
x_i / g/g								
FA	0.509	-	0.616	0.264	0.806	0.428	0.003	0.560
WA	0.286	0.010	0.344	0.637	0.141	0.409	0.997	0.100
ME	0.205	0.990	0.040	0.100	0.053	0.163	-	0.340

Table 11: Unit operations data Process III, Route 4

Unit:	T/°C	p / bar	$\dot{Q}$ / kW
TFE	118.12	0.20	359.30
CON_1	57.94	0.20	-373.22

Table 12: Columns Process III, Route 4

Distillation columns	C_1	C_2
$\dot{Q}_{top}$ / kW	-830.89	-580.75
T_{top}/°C	47.84	135.22
$\dot{Q}_{bot}$ / kW	506.07	663.77
T_{bot}/°C	83.43	143.67
p / bar	0.50	4.00
N	28.00	22.00
N^{Feed}	16.00	14.00
RR	6.13	2.60

1.1.4. Process III, Thin-film evaporation*

Mantei et al. [11] previously suggested a simpler FA concentration based on thin-film evaporation. In their work, two thin-film evaporators are employed to produce OME feedstock, cf. Figure 4. The process is adopted without modification; the complete stream table and PFD were provided by Mantei et al. [11].

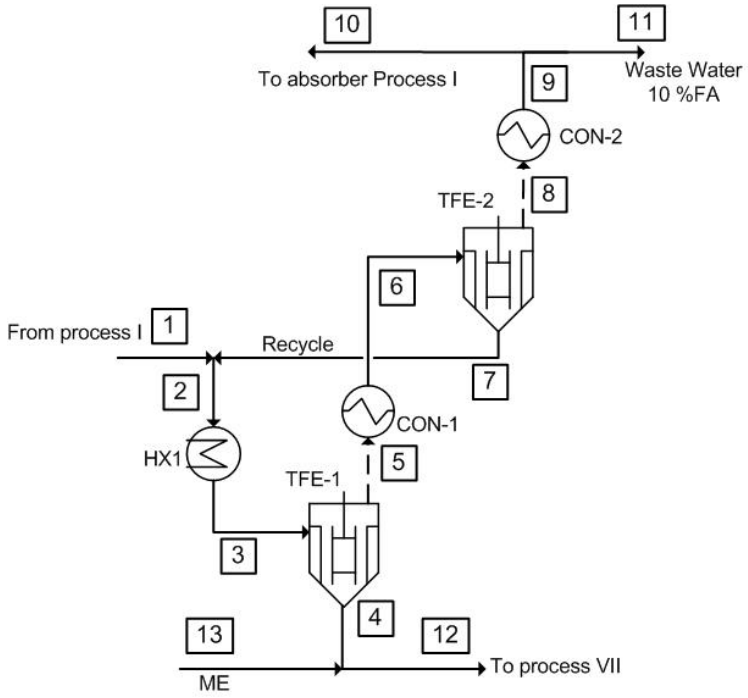

Figure 4: PFD of Process III* adopted from Mantei et al. [11].

The aqueous FA solution from Process I (1) is preheated, fed to TFE1, concentrated to 0.86 g/g FA (4), and mixed with ME to produce OME feedstock (8). The top product of TFE1 (5) is condensed and fed to TFE2. The bottom product of TFE2 (7) is recycled and mixed with the feed. The top product (8) is condensed, and part of it is recycled to Process I to be used as an absorbent in the absorber; part of it is removed as wastewater. The material and energy balance was adopted from Mantei et al. [11]. 8 wt% of all fed FA is lost in the wastewater stream (11). Tables 13 to 14 give the stream table and unit data of the process.

Table 13: Stream Table Process III*

Stream	1	2	3	4	5	6	7	8	9	10	11	12	13
$\dot{m}$ / kg/h	1364.86	1598.12	1598.12	723.76	874.36	874.36	233.26	641.10	641.10	88.22	552.88	1099.42	375.66
p / bar	0.07	0.07	0.07	0.07	0.07	0.20	0.20	0.20	0.20	1.00	1.00	1.00	1.00
T/°C	44.83	45.30	50.00	50.00	50.00	40.00	40.00	40.00	30.00	30.12	30.12	25.00	25.00
x_i / g/g													
FA	0.503	0.537	0.537	0.860	0.269	0.269	0.731	0.101	0.101	0.101	0.101	0.566	-
WA	0.490	0.458	0.458	0.137	0.723	0.723	0.269	0.888	0.888	0.888	0.888	0.090	-
ME	0.007	0.006	0.006	0.003	0.008	0.008	-	0.011	0.011	0.011	0.011	0.344	1.000

Table 14: Unit operations data Process III*

Unit:	T/°C	p / bar	$\dot{Q}$ / kW
HX_1	50.00	0.07	136.83
TFE_1	50.00	0.20	415.45
CON_1	40.00	0.20	-382.52
TFE_2	40.00	0.20	282.35
CON_2	40.00	0.20	-434.56

1.1.5. Process IV, Pervaporation

Pervaporation has been successfully applied for the removal of water from various organic solvents, for example, ethanol [12, 13] and has been suggested for the removal of water from aqueous and methanolic FA solutions in patent literature [14, 15]. Furthermore, it has been proven in lab-scale experiments that pervaporation can be used to remove water from a stream composed of FA, WA, ME, and OME in the OME production process. In the referred study [16] suitable membrane materials have been identified regarding flux, permeate purity, and stability. Figure 3 shows a PFD for a pervaporation unit based on these works considered here for the removal of water from FA solutions.

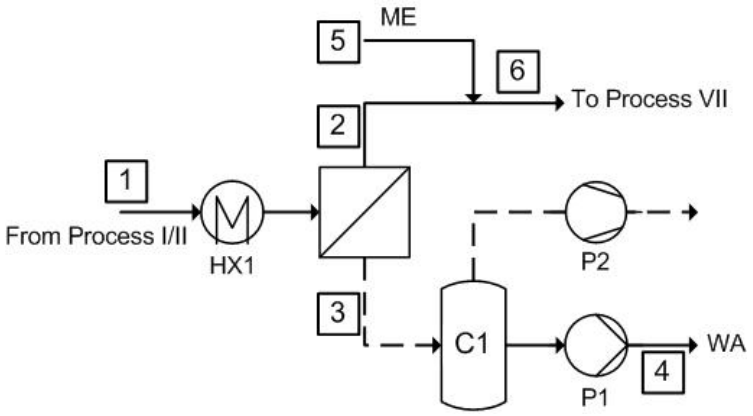

Figure 5: PFD of the pervaporation unit including utility.

FA solution (1) is preheated in HX1 and fed to the membrane module M1 equipped with a hydrophilic polymeric membrane, PERVAP 4101 [16]. The pressure at the permeate side has to be sufficiently low to provide enough driving force; a pressure of 0.032 bar is chosen here. The water passes through the membrane to the permeate side; the module is adiabatic. The vapor (3) is condensed in CON1. The pump P1 conveys the condensed water, and a small auxiliary compressor attached to CON1 removes traces of inert gas. We assume the permeate has the same composition as in the original work [16] (**0.984 g/g** water). The retentate is mixed with methanol to produce OME feedstock. The permeate mass flow rate determines the remaining mass fraction of water in the retentate leaving the pervaporation unit (i.e., the produced OME feedstock). It influences both the heat demand and the required membrane surface in process IV and the subsequent OME process VII. In a sensitivity study, the water content in the OME feedstock was varied in both processes. The overall heat demand is calculated in process simulation; the required membrane surface area is calculated from the correlation given by Schmitz et al. [16]. All other process parameters besides the water content in the retentate are kept constant. Figure 6 gives the resulting trade-off between membrane area and heat demand.

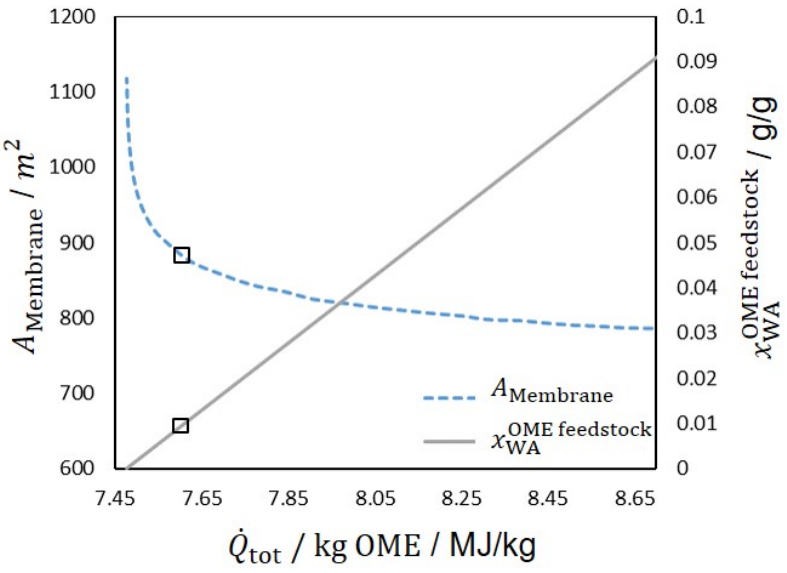

Figure 6: Membrane surface area and heat demand per kg OME in Process IV and in the OME process. The solid line shows the water fraction in the OME feedstock, and the dashed line the membrane surface area. The rectangles show the chosen operating point for the pervaporation unit.

The heat demand in the OME process increases significantly with higher water contents. This

is because water inhibits OME formation in the reactor, leading to bigger recycle streams. The operating point (OP) for the pervaporation unit is chosen at $x_{\mathrm{WA}}^{\mathrm{OME\ feedstock}}$=0.01 g/g where both area and heat demand are close to their minima. Lower water contents are not advisable as they would lead to drastically higher membrane surfaces areas while saving little heat.
Depending on the setup of the plant, multiple pervaporation units can be employed in sequence to achieve the required membrane surface. In this case, HX1 serves as an intermediate heater to keep the retentate/feed at a constant operating temperature. Currently, the required membranes are not manufactured on a large scale, and estimating the future costs based on the limited information is difficult. In this work, the membrane housing cost is estimated to 50 $\$/m^2$ and the membrane cost to 200 $\$/m^2$ [17, 13, 18]. Tables 15 to 16 give the stream table and unit data of the process for Route 2, tables 17 to 18 for Route 5 and tables 19 and 20 for Route 6.

Table 15: Stream Table Process IV, Route 2

Stream	1	2	3	4	5	6
$\dot{m}$ / kg/h	1252.31	636.45	615.85	615.85	373.65	1010.10
p / bar	1.00	1.00	**0.03**	0.03	1.00	1.00
T/°C	65.61	65.61	65.61	**25.00**	25.00	25.00
x_i / g/g						
FA	0.505	0.978	**0.016**	0.016	-	0.616
WA	0.492	0.016	**0.984**	0.984	-	**0.010**
ME	0.003	0.007	-	-	1.000	0.374

Table 16: Unit operations data Process IV, Route 2

Unit:	T/°C	p / bar	$\dot{Q}$ / kW
HX1	65.61	0.03	403.54
CON1	25.00	0.03	-428.48

Table 17: Stream Table Process IV, Route 5

Stream	1	2	3	4	5	6
$\dot{m}$ / kg/h	1233.93	885.56	348.37	348.37	124.54	1010.10
p / bar	1.00	1.00	**0.03**	0.03	1.00	1.00
T/°C	69.50	69.50	69.50	**25.00**	25.00	25.00
x_i / g/g						
FA	0.509	0.703	**0.016**	0.016	-	0.616
WA	0.286	0.011	**0.984**	0.984	-	**0.010**
ME	0.205	0.286	-	-	1.000	0.374

Table 18: Unit operations data Process IV, Route 5

Unit:	T/°C	p / bar	$\dot{Q}$ / kW
HX_1	25.14	0.03	195.51
CON_1	25.00	0.03	-213.74

Table 19: Stream Table Process IV, Route 6

Stream	1	2	3	4	5	6
$\dot{m}$ / kg/h	670.94	369.23	301.72	301.72	213.40	582.62
p / bar	1.00	1.00	**0.03**	0.03	1.00	1.00
T/°C	99.20	99.20	99.20	**25.00**	25.00	25.00
x_i / g/g						
FA	0.542	0.972	**0.016**	0.016	-	0.616
WA	0.451	0.016	**0.984**	0.984	-	**0.010**
ME	0.007	0.012	-	-	1.000	0.374

Table 20: Unit operations data Process IV, Route 6

Unit:	T/°C	p / bar	$\dot{Q}$ / kW
HX_1	69.50	0.03	190.30
CON_1	25.00	0.03	-218.06

1.1.6. Process V: Extractive distillation

A patent by Morishita et al. [19] suggests the production of gaseous FA of high purity from an aqueous FA solution via extractive distillation. Figure 7 shows the PFD of the process. Columns C2 and C3 and the compositions of their feed and product streams are adopted from the original work without changes; the recycle (6), column C1, evaporator E1, and absorber A1 were added in the present work. The compositions of the feed, top, and bottom products of the extractive distillation column as well as its size are adopted from the original literature. Aqueous FA solution (1) is pre-concentrated in distillation column C1, and pure water (0.997 g/g) is removed at the bottom of C1. The top product (2) contains 0.65 g/g FA [19] and is fed to the lower part of the extractive distillation column C2. In the upper part of the column, a large stream of polyethylene glycol dimethyl ether (PEG) is added as an extracting agent at a temperature of 120 °C. Column C2 is equipped with a reboiler operated at 170 °C; there is no condenser at the top. Pure gaseous FA is recovered from the top as stream (4). In order to produce OME-feedstock, we added a loss-free absorption of this gaseous FA in ME in absorber A1. Column C2's bottom product (5), comprised of PEG, water, and FA, is separated in column C3. We assume that PEG can be sharply separated from WA in distillation as bottom product (7) due to its low vapor pressure. Dilute aqueous FA solution (6) is removed at the top and recycled to convert all FA to OME feedstock. E1 evaporates and removes a small purge stream (8) to prevent an accumulation of small amounts of ME.

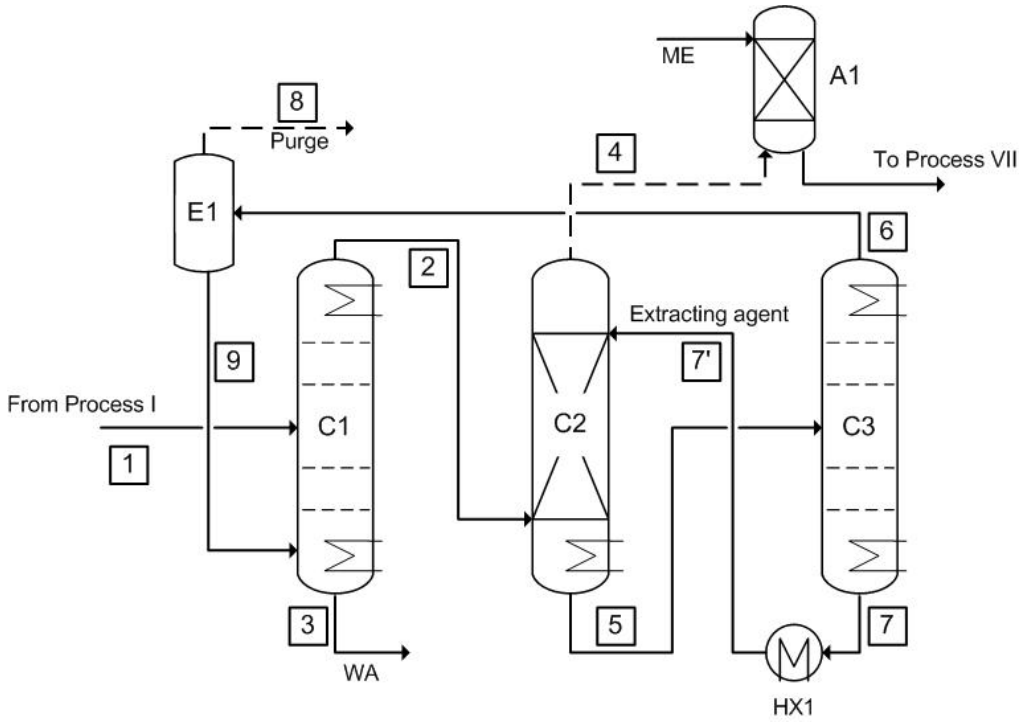

Figure 7: PFD of the extractive distillation process based on Morishita et al. [19].

There is no property model readily available for the extracting agent. However, since there is no PEG present in C1, E1, and A1, the energy demand of these units is calculated via process simulation using the described model for FA, ME, WA. The energy demand of column C2 is trivially calculated since it has no condenser and the material balance and the heat capacity of PEG are available. For column C3 the condenser duty $\dot{Q}_{\mathrm{C}}$ is estimated from the enthalpy of vaporization $\Delta h_{v,i}(T)$ of the components of the top product, their mass flow rate $\dot{m}_i$, and the reflux ratio RR:

$$\dot{Q}_{\mathrm{C}} = (RR + 1) \cdot \sum_{i=1}^{N} (\Delta h_{v,i}(T) \cdot \dot{m}_i) \tag{1}$$

The reflux ratio of C3 is estimated as 1.44 based on Underwood's equation using a relative volatility of WA/PEG of 230 [20]. The reboiler duty $\dot{Q}_{\mathrm{B}}$ is calculated via the energy balance of the whole column

$$\dot{Q}_{\mathrm{B}} = \dot{H}_{\mathrm{Bottom}} + \dot{H}_{\mathrm{Top}} - \dot{H}_{\mathrm{Feed}} - \dot{Q}_{\mathrm{C}} \tag{2}$$

with $\dot{H}_{\text{Bottom}}$, $\dot{H}_{\text{Top}}$, $\dot{H}_{\text{Feed}}$ being the enthalpy streams of bottom product, top product, and feed, respectively. Tables 21 to 23 give the stream table and unit data of the process.

Table 21: Stream Table Process V

Stream	1	2	3	7'	4	5	6	7	8	9	10
$\dot{m}$ / kg/h	1251.19	1150.47	602.77	23009.42	623.15	23534.24	526.54	23009.42	24.50	502.05	1000.00
p / bar	6.00	**6.00**	**6.00**	2.00	**2.00**	**2.00**	2.00	**2.00**	2.00	2.00	2.00
T/°C	65.94	137.60	158.63	120.00	**120.00**	**170.00**	113.38	**170.00**	114.92	114.92	110.00
x_i / g/g											
FA	0.504	**0.650**	0.003	-	**1.000**	**0.005**	0.237	-	0.328	0.236	0.623
WA	0.492	0.318	**0.997**	-	-	**0.017**	0.694	-	0.511	0.700	-
ME	0.003	0.032	-	-	-	**-**	0.069	-	0.161	0.064	0.377
PEG	-	**-**	-	1.000	-	**0.978**	**-**	**1.000**	-	-	-

Table 22: Unit operations data Process V

Unit:	T/°C	p / bar	$\dot{Q}$ / kW
E_1	114.92	2.00	12.37
HX_1	120.00	2.00	-694.92
A_1	110.00	6.00	-251.98
HX_2	40.00	1.00	-391.52

Table 23: Columns Process V

Distillation colmns	C_1	C_2	C_3
$\dot{Q}_top$ / kW	-1285.78	-	-417.13
T_top/°C	137.60	-	113.38
$\dot{Q}_bot$ / kW	1468.70	992.10	348.69
T_bot/°C	158.63	**170.00**	**170.00**
N	24.00	**49.00**	**43.00**
N^{Feed}	11.00	-	-
$N^{Feed(9)}$	20.00	-	-
p / bar	**6.00**	**2.00**	**2.00**
RR	1.42	-	1.44

1.1.7. Process VI: Chemical separation of water and extractive distillation

A process proposed by Masamoto et al. [21] is based on the production of the intermediate MAL in order to remove pure WA. Figure 8 gives the PFD of the process.

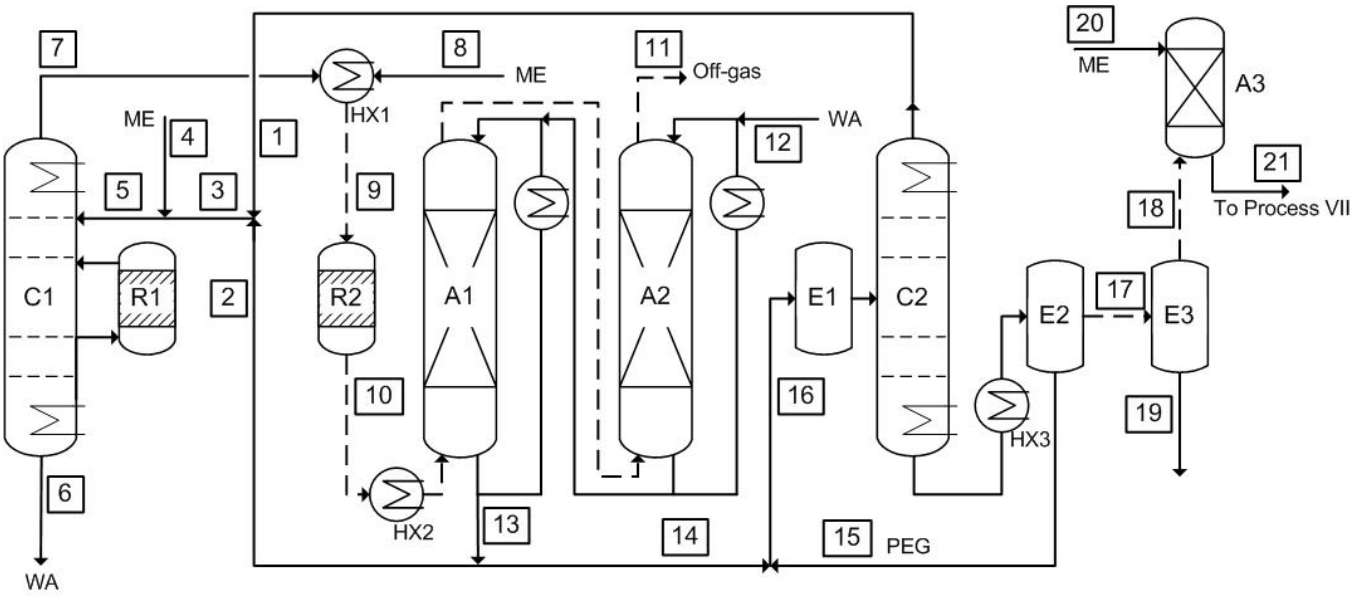

Figure 8: PFD of process proposed by Masamoto et al.

An aqueous solution of 0.39 g/g FA (3) produced in this process is mixed with ME (4) and fed to distillation column C1 as stream (5). Sidestreams of C1 are fed to three reactors (only one reactor shown, cf. R1), where MAL is formed and recycled to the column and subsequently removed at the top as stream (7) (0.90 g/g MAL 0.1 g/g ME). Pure water is removed as bottom product (6). Stream (7) is combined with air (8) and fed to reactor R2 to produce FA. The reactor product (10) is absorbed in absorption columns A1 and A2 to produce a concentrated aqueous solution of 0.65 g/g FA (13). Part of stream (13) is recycled as stream (2).

The other part (14) is mixed with an extracting agent (PEG) (15) in the stirred vessel E1 and subsequently fed to column C2. In C2, a dilute aqueous FA solution of 27% FA is removed as the top product (1) and recycled. The bottom product of C2 is fed to the flash vessel E2, where pure PEG is recovered as a liquid product (15). The gaseous product (17) is fed to cooling trap E3, where pure FA gas is removed as stream (18), and small amounts of water and ME are removed as stream (19). The gaseous FA is absorbed in ME in Absorber A3 to produce OME feedstock. The recycled streams (2) and (1) form the aqueous FA solution (3) that is part of the feed. The absorbers A1 and A2 are modeled with 3 and 4 vapor-liquid equilibrium (VLE) stages, respectively. A liquid solution is drawn at the bottom of each absorber, cooled, and recycled to its top. The

distillation column C1 is simulated rigorously using the described property model. The adiabatic reactors ascribed to it are modeled considering the chemical equilibrium reactions 6 and 9 in the main manuscript and the formation of MAL from FA and ME [22]. They draw and recycle solutions at stages 15, 18, and 21. Due to missing property data for PEG, column C2 is not simulated, but its heat demand is estimated based on the enthalpy of vaporization of the top product, the top and bottom product mass flow rates $\dot{m}_i$, and the reflux ratio, cf. section 1.1.6 for details. A reflux ratio of 1.4 was assumed. All stream compositions are adopted from the original work [21], tables 24 to 25 give the stream table and unit data of the process.

Table 24: Stream Table Process VI

Stream	1	2	3	4	5	6	7	8	9	10	11	12	13	14	15	16	17	18	19	20	21
$\dot{m}$ / kg/h	539.51	242.41	781.92	735.60	1510.61	655.24	858.02	7614.94	8472.96	8472.96	7560.47	497.90	1410.40	1167.99	1594.82	3720.44	628.48	611.92	16.56	388.08	1000.00
p / bar	1.00	1.00	1.00	1.00	1.00	1.00	1.00	1.00	1.00	1.00	1.00	2.00	1.00	1.00	1.00	1.00	1.00	1.00	1.00	1.00	1.00
T/°C	56.33	67.30	59.99	25.00	59.86	99.62	41.58	25.00	40.00	340.00	39.98	25.00	67.30	67.30	140.00	96.47	140.00	-	-	25.00	25.00
x_i / g/g																					
FA	**0.273**	0.650	0.390	-	0.202	0.001	-	-	-	**0.111**	**0.003**	-	**0.650**	0.650	-	0.372	**0.973**	**0.999**	-	-	0.612
WA	0.718	0.346	0.602	-	0.311	**0.999**	-	**0.013**	0.011	**0.039**	0.045	**1.000**	**0.346**	0.346	-	0.196	0.026	-	0.998	-	-
ME	0.009	0.004	0.008	1.000	0.487	-	**0.101**	-	0.010	**0.003**	0.002	-	0.004	0.004	-	0.003	-	-	-	1.000	0.388
CO_2	-	-	-	-	-	-	-	-	-	-	-	-	-	-	-	-	-	-	-	-	-
N_2	-	-	-	-	-	-	-	**0.897**	0.807	0.807	0.904	-	-	-	-	-	0.001	0.001	-	-	-
O_2	-	-	-	-	-	-	-	**0.090**	0.081	0.037	0.042	-	-	-	-	-	-	-	-	-	-
H_2	-	-	-	-	-	-	-	-	-	-	-	-	-	-	-	-	-	-	-	-	-
CO	-	-	-	-	-	-	-	-	-	0.003	0.003	-	-	-	-	-	-	-	-	-	-
MAL	-	-	-	-	-	-	**0.899**	-	0.091	**0.001**	0.001	-	-	-	-	-	-	-	0.002	-	-
PEG	-	-	-	-	-	-	-	-	-	-	-	-	-	-	1.000	0.768	-	-	-	-	-

Table 25: Unit operations data Process VI

Unit:	T/°C	p / bar	$\dot{Q}$ / kW
HX_{1_1}	140.00	1.00	71.44
HX_{3_1}	40.00	1.00	137.78
R_2	340.00	1.00	41.85
E_1	79.98	1.00	-57.82
E_2	79.98	1.00	353.97
E_3	0.00	1.00	-42.06
A_1	67.30	1.00	510.71
A_2	39.98	1.00	-750.91
A_3	25.00	1.00	-418.61

Distillation columns	C_1	C_2
$\dot{Q}_{top}$ / kW	-321.59	-340.30
T_{top}/°C	41.58	56.33
$\dot{Q}_{bot}$ / kW	306.88	325.71
T_{bot}/°C	99.62	79.98
p / bar	1.00	1.00
N	32.00	**10**
N^{Feed}	15.00	**1**
RR	2.05	1.40

1.1.8. Process VII: OME production

The OME production process is adopted from Schmitz et al. [23]. All compositions and mass flow rates are adopted without modifications, Figure 9 gives a PFD.

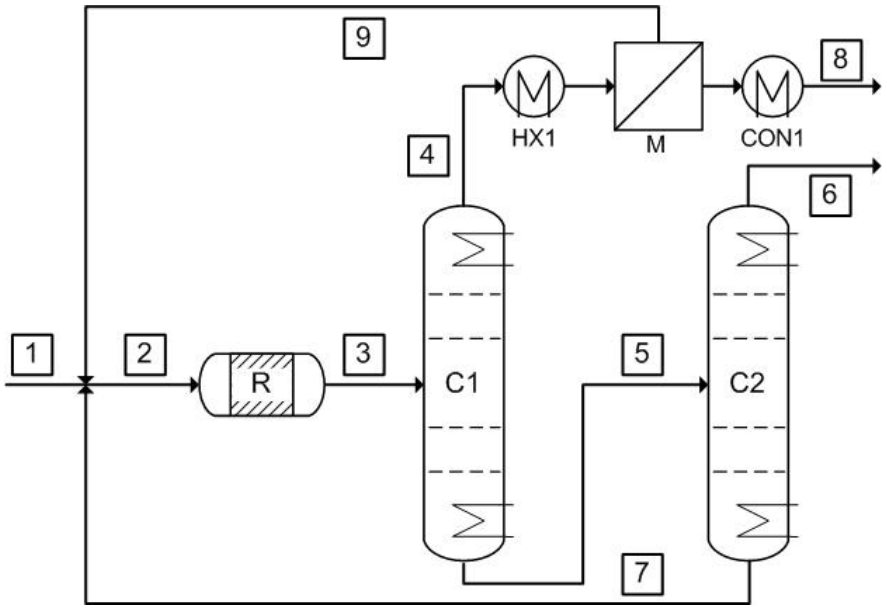

Figure 9: PFD of the OME process proposed by Schmitz et al. [23].

The OME feedstock is mixed with the recycle streams 7 and 9 and fed to the isothermic reactor R. R is operated at 68 °C and 2 bar and is filled with Amberlyst 46 as a catalyst. 0.277 kg of catalyst is required per kg of produced OME_{3-5} per hour. The reactor product (3) is fed to distillation column C1, where OME_3 and all longer chained OME are yielded in the bottom product.
The bottom product (5) is fed to column C2, where all $OME_{n>5}$ is separated as the bottom product (7) and recycled, the top product (6) is the product OME_{3-5}. The top product of C1 (4) is fed to a pervaporation unit M1 to remove pure water (8) as permeate. The retentate (9) is recycled to the reactor. Tables 26 to 28 give the stream table and unit data of the process. Note that the process data is given exemplary for route 4, where 0.10 g/g of water is present in the OME Feedstock. However, the OME process has been simulated with the corresponding amount of water in the feed for every route.

Table 26: Stream Table Process VII

Stream	1	2	3	4	5	6	7	8	9
$\dot{m}$ / kg/h	1111.10	8101.00	8100.99	7145.08	955.92	893.78	62.13	217.31	6927.77
p / bar	1.00	**2.00**	**2.00**	**1.40**	**1.40**	**0.10**	**0.10**	1.40	1.40
T/°C	70.00	68.51	68.00	68.27	184.97	96.41	202.71	68.27	68.27
x_i / g/g									
FA	0.560	0.207	0.130	0.148	-	-	-	-	0.152
WA	0.100	0.018	0.031	0.036	-	-	-	1.000	**0.005**
ME	0.340	0.153	0.106	0.120	-	-	-	-	0.124
MAL	-	0.393	0.393	0.445	-	-	-	-	0.459
OME_2	-	0.195	0.195	0.221	-	-	-	-	0.228
OME_3	-	0.027	0.086	**0.030**	**0.502**	0.536	-	-	0.031
OME_4	-	-	0.036	-	0.302	0.323	-	-	-
OME_5	-	-	0.014	-	0.121	0.129	-	-	-
OME_6	-	0.004	0.006	-	0.047	**0.011**	**0.567**	-	-
OME_7	-	0.002	0.002	-	0.018	-	0.276	-	-
OME_8	-	0.001	0.001	-	0.007	-	0.104	-	-
OME_9	-	-	-	-	0.003	-	0.039	-	-
OME_10	-	-	-	-	0.001	-	0.014	-	-

Table 27: Unit operations data Process VII

Unit:	T/°C	p / bar	$\dot{Q}$ / kW
R	68.00	2.00	-39.06
HX_1	68.27	1.40	114.64
CON_1	5.46	0.03	-157.08

Table 28: Columns Process VII

Distillation columns	C_1	C_2
$\dot{Q}_{top}$ / kW	-1597.75	-162.49
T_{top}/°C	68.27	96.41
$\dot{Q}_{bot}$ / kW	1656.66	119.21
T_{bot}/°C	184.97	202.71
p / bar	**1.40**	**0.10**
N	13.00	13.00
N^{Feed}	7.00	6.00

2. Model of physico-chemical properties

2.1. FA production and concentration

Correlations for the vapor pressures (MAL[24], FA[24], MG_n[24], HF_n[24], WA[24]) were adopted from literature. The same holds for enthalpies of vaporization (FA[25], MAL [25], ME[26], WA[26], FA [26]) and the ideal gas heat capacities (FA[25], MAL [25], ME [26], WA[26], FA [26]). Enthalpies of formation are adopted from the literature as well (FA[25], MAL[25], ME[24], WA[24]). The UNIFAC parameters of the activity model for the system WA, FA, ME, MG, HF, MAL are adopted from Kuhnert et al. [24]. The activity-based equilibrium constants K_a of the formation of MG_n and HF_n are adopted from Kuhnert et al. [24]. For thin-film evaporators, the reaction kinetics in the liquid phase are modeled as described by Ott et al. [22]. For the noncondensable gases N_2, O_2, CO, CO_2, H_2, property data for vapor pressures, enthalpies of formation in the gas phase, enthalpies of vaporization, ideal gas heat capacities are adopted from the DIPPR database [25]. Gas solubilities are neglected for these components. We found no consistent enthalpy model readily available for the MG_n and HF_n. Therefore one is derived based on their vapor pressure and the activity-based equilibrium constants K_a of the formation of MG_n and HF_n [24]. A similar procedure to the following for the derivation of this enthalpy model has already been described by Bongartz et al. [27].

All specific enthalpies are normalized to the enthalpy of formation $h_i^f(T^\theta)$ in the gaseous state at standard temperature T^θ and are calculated based on the following equations :

$$h_i(T_1) = h_i^f(T^\theta) + \int_{T^\theta}^{T_1} c_{p,i}^g dT \tag{3}$$

for gasoues streams, and

$$h_i(T_1) = h_i^f(T^\theta) + \int_{T^\theta}^{T_1} c_{p,i}^g dT - \Delta h_{v,i}(T_1) \tag{4}$$

for liquid streams. Pressure dependence of the enthalpies is neglected. $c_{p,i}^l$ and $c_{p,i}^g$ are the isobaric, specific heat capacities in the liquid and gaseous phase, respectively. $\Delta h_{v,i}$ denotes the enthalpy of vaporization.

The enthalpy of vaporization of MG_1 and HF_1 is estimated from their vapor pressure via the Clausius Clapeyron equation assuming an ideal gas phase and neglible liquid volume

$$\frac{1}{p} dp = \frac{\Delta h_{v,i}}{RT^2} dT. \tag{5}$$

The reaction enthalpies $\Delta_R h(T)$ of Reactions (1)-(4) in the main article for the formation of MG/HF in the liquid phase are calculated from the respective equilibrium constant K_a via the Van-'t-Hoff-equation:

$$\left(\frac{\partial \ln K_a}{\partial T} \right) = \frac{\Delta_R h(T)}{RT^2}. \tag{6}$$

The specific enthalpies of all MG/HF species in the liquid phase

$$h^{liq}_{\mathrm{MG}_n}(T) = \Delta^{liq}_R h_{\mathrm{MG}_n}(T) + h^{liq}_{\mathrm{MG}_n-1}(T) + h^{liq}_{\mathrm{FA}}(T) \tag{7}$$

(HF analogously) and the enthalpies of MG_1 and HF_1 in the gaseous phase are calculated for multiple temperatures in the range of 298.15 K to 415.15 K. This also yields the standard enthalpies of formation (at 298.15 K) for MG_1 and HF_1 in the gaseous phase and $MG/HF_{n¿1}$ in the liquid phase. Heat capacities are fitted for MG_1 and HF_1 in the gaseous phase and $MG/HF_{n¿1}$ in the liquid phase so that the enthalpies in the temperature range can be calculated using Eq. (4) instead of Eq. (7). The heat capacities are fitted to a polynomial that meets the required input format of Aspen:

$$c_p/\mathrm{J/molK} = A + BT + CT^2 + DT^3 + ET^4. \tag{8}$$

The enthalpies of $MG/HF_{n¿1}$ in the gas phase are not required since they are assumed to be always liquid due to their very low vapor pressure. The critical temperatures $T_c(MG_1)$ and $T_c(HF_1)$ are estimated with the method of Lyderson. Parameters for all used correlations are given in the first author's dissertation [10].

2.2. Property data Process VII

The property model used for the OME process is adopted from Schmitz [28], which has slight differences to the model used in process I-VI.

3. Assumptions Techno-Economic Assessment

Tables 29 to 32 give the assumption and sources for the Techno-Economic Assessment of Routes 1-7.

Table 29: Factors for CAPEX and OPEX estimation based on Peters et al. [29].

Factors for CAPEX estimation	Factor	Basis
Direct Investment Costs		
Equipment costs	1	EQ costs
Installation	0.47	EQ costs
Instrumentation and controls	0.36	EQ costs
Piping	0.68	EQ costs
Electrical systems	0.11	EQ costs
Buildings	0.18	EQ costs
Yard improvements	0.1	EQ costs
Service facilities	0.7	EQ costs
Indirect Investment Costs		
Engineering and supervision	0.33	EQ costs
Contruction expenses	0.41	EQ costs
Legal expenses	0.04	EQ costs
Contractor's fee	0.22	EQ costs
Contingency	0.44	EQ costs
Fixed Capital Investment (FCI)	5.04	EQ costs
Working Capital (% of TCI)	15%	TCI
Total Capital Investment (TCI)	5.93	EQ costs
Factors for OPEX estimation		
Direct Operating Costs		
Insurance and taxes	0.02	FCI
Maintenance labor (ML)	0.01	FCI
Maintenance material (MM)	0.01	FCI
Operating supplies (OS)	0.15	ML+MM
Operating supervision (OV)	0.15	OL
Laboratory charges	0.2	OL
Plant overhead costs (PO)	0.5	OL+OV+OS
Administrative costs	0.25	PO
Distribution and selling costs	0	NPC
Research and development costs	0	NPC

Table 30: Further boundary conditions for economic estimation and further estimation factors

	Value	Base	Reference
Economic Parameters			
Reference year	2018		
Operating hours per year	8000		
Depreciation period in years	20		
WACC	0.05		
Annuity	0.08	FCI	
Material Factors			
Carbon steel	1		[29]
Aluminium and bronze	1.07	Carbon steel Equipment	[29]
Cast steel	1.1	Carbon steel Equipment	[29]
304 stainless steel	1.3	Carbon steel Equipment	[29]
316 stainless steel	1.3	Carbon steel Equipment	[29]
321 stainless steel	1.5	Carbon steel Equipment	[29]
Hastelloy C	1.55	Carbon steel Equipment	[29]
Monel	1.65	Carbon steel Equipment	[29]
Nickel and Inconel	1.7	Carbon steel Equipment	[29]
Location Factors			
United States Gulf Coast	1		[29]
Germany	1.11	Equipment cost US Gulf Coast	[29]
Chemical Engineering Plant Cost Index			
Jan 10	532.9		[30]
2018	603.1		[30]
2019	607.5		[30]
Exchange Rate			
EUR/USD (2018)	0.846383808		[31]

Table 31: Direct Costs for OPEX estimation

	Value	Unit	Reference
Raw Materials			
Methanol	401.75	EUR/t	[32]
Water	1	EUR/t	Own assumption
Air	0		Own assumption
Utility Costs			
Power	50	EUR/MWh	Own assumption
Natural gas	28.2	EUR/MWh	[33]
Cooling water	0.005	EUR/kWh	Own assumption
Steam 4 bar, 150°C	22.8	EUR/t	Based on Turton [34]
Steam 20 bar, 220 °C	23.1	EUR/t	Based on Turton [34]
Steam 70 bar, 290 °C	23.5	EUR/t	Based on Turton [34]
Cooled water	0.0075	EUR/kWh	Own assumption
Cooling Agend (Salt Solution)	0.015	EUR/kWh	Own assumption
Consumables			
Catalyst	700	EUR/kg	Own assumption
Extraction agent	2996.19	EUR/t	[21]
Labor costs			
Hourly wages	41.91	EUR/h	Own assumption

Table 32: Heat Transfer coefficients[35]

Type	Value	Unit
Shell-and-tube heat exchangers		
- without phase change -		
Gas (1 bar) inside - Gas (1 bar) outside	20	$W/m^2 K$
Gas (200 bar) inside - Gas (200 bar) outside	325	$W/m^2 K$
Liquid - Gas (1 bar)	42.5	$W/m^2 K$
Gas, high pressure (200 bar) inside - Liquid outside	300	$W/m^2 K$
Liquid inside - Liquid outside	625	$W/m^2 K$
Superheated steam outside - Liquid inside	750	$W/m^2 K$
- Evaporator -		
Natural circulation - low viscosity	600	$W/m^2 K$
Natural circulation - high viscosity	1250	$W/m^2 K$
Forced circulation	2000	$W/m^2 K$
- Condenser -		
Cooling water inside - Steam outside	750	$W/m^2 K$
Waste heat boiler		
Gas inside - Boiling water outside	32.5	$W/m^2 K$
Double pipe		
Gas (1 bar) inside - Gas (1 bar) outside	22.5	$W/m^2 K$
Gas (200 bar) inside - Gas (1 bar) outside	40	$W/m^2 K$
Gas (200 bar) inside - Gas (200 bar) outside	325	$W/m^2 K$
Gas, high pressure (200 bar) inside - Liquid outside	400	$W/m^2 K$
Liquid inside - Liquid outside	850	$W/m^2 K$
Plate heat exchanger		
Flat channels — Gas - Water	40	$W/m^2 K$
Flat channels — Liquid - Water	575	$W/m^2 K$
Profile plates — Liquid - Liquid	2500	$W/m^2 K$
Cooling		
Min temperature Difference 27	10	K
Heating		
Steam Network available		
Boiling Water at pressure level of steam network available		

Abbreviations

A	Absorber
B	Burner
C	Column
CAPEX	Capital Expenditure
CEPCI	Chemical Engineering Plant Cost Index
CON	Condenser
DME	Dimethylether
E	Various unit operations with phase change
FA	Formaldehyde
HF_n	Poly(oxymethylene) hemiformal
HX	Heat exchanger
LPC	Levelized product cost
M	Membrane Unit
MAL	Methylal
MCO	Multi-criteria optimization
ME	Methanol
MG_n	Poly(oxymethylene) glycol
OME_n	Poly(oxymethylene) dimethyl ether of chain length n
OP	Operating point
OPEX	Operational Expenditure
PEG	Polyethylene glycol dimethyl ether
PFD	Process flow diagram
R	Reactor
RR	Reflux Ratio
SI	Supporting Information
TFE	Thin Film Evaporator
TRI	Trioxane
TRL	Technology Readiness Level
VLE	Vapor-liquid equilibrium
WA	Water
WACC	Weighted Average Cost of Capital

Variables

A	Surface
c	Cost
c_p	Isobaric heat capacity
$\Delta h_{v,i}$	Enthalpy of vaporization
$\Delta h_{R,i}$	Reaction enthalpy
H	Enthalpy
h_i	Specific enthalpy of component i
h_i^f	Standard enthalpy of formation of component i
K	Number of components
k	Heat transfer coefficient
$\dot{m}$	Masss flow rate
N	Number of stages
n	Chain length
p	pressure
$\dot{Q}_i$	Heat duty of unit i
$\dot{Q}_{tot}$	Total heat duty
R	Universal gas constant
T	Temperature
T_c	Critical temperature
x_i^k	Mass fraction of component i in k

Acknowledgements

This study was carried out in the framework of the E2Fuels project (project no.: 03EIV011G) funded by the German Federal Ministry for Economic Affairs and Energy. The financial support is gratefully acknowledged.

The authors acknowledge the cooperation within the Network TUM.Hydrogen and PtX.

References

[1] G. Reuss, W. Disteldorf, A. O. Gamer, A. Hilt, Formaldehyde, in: Ullmann's Encyclopedia of Industrial Chemistry, Wiley-VCH Verlag GmbH & Co. KGaA, Weinheim, Germany, 2000.

[2] V. Schröder, Explosionsgrenzen von Wasserstoff und Wasserstoff/Methan-Gemischen, Tech. rep., Bundesanstalt für Materialforschung und -prüfung (BAM) (2002).

[3] X. Liu, Y. Huang, Y. Wang, Q. Zhang, Critical explosible oxygen concentration of methanol-saturated vapor/O 2/N2 mixtures at elevated temperatures and pressures, Industrial and Engineering Chemistry Research 53 (13) (2014) 5617–5621. doi:10.1021/ie402502j.

[4] M. Qian, M. A. Liauw, G. Emig, Formaldehyde synthesis from methanol over silver catalysts, Applied Catalysis A: General 238 (2) (2003) 211–222. doi:10.1016/S0926-860X(02)00340-X.

[5] L. Eek Vancells, Method for producing stabilized solutions of formaldehyde with methanol. Patent EP0434783B1 (1990).

[6] D. L. Kloepper, L. G. Stevenson, Method for making alcoholformaldehyde product. Patent US3214891A (sep 1965).

[7] E. Ströfer, N. Lang, U. Lichtfers, U. Steinbrenner, H. Hasse, Separation of liquid mixtures in a film evaporator. Patent US7414159B2 (mar 2003).

[8] E. Ströfer, T. Gruetzner, H. Hasse, N. Lang, M. Ott, Verfahren zur erzeugung hochkonzentrierter formaldehydlösungen. Patent WO2004078678A3 (2003).

[9] K. Schilling, M. Sohn, E. Ströfer, H. Hasse, Reaktive Verdampfung formaldehydhaltiger Mischungen und Process Monitoring mit Online-NMR-Spektroskopie, Chemie Ingenieur Technik 75 (3) (2003) 240–244. doi:10.1002/cite.200390047.

[10] Y. Tönges, Advances in the production of poly(oxymethylene) dimethyl ethers and methanolic formaldehyde solution, Phd thesis, Technical University of Munich (2022).

[11] F. Mantei, R. E. Ali, C. Baensch, S. Voelker, P. Haltenort, J. Burger, R.-U. Dietrich, N. Von Der Assen, A. Schaadt, J. Sauer, O. Salem, Techno-economic assessment and Carbon footprint of processes for the large-scale production of Oxymethylene Dimethyl Ethers from Carbon Dioxide and Hydrogen, Sustainable Energy & Fuels 6 (2021) 528–549. doi:10.1039/D1SE01270C.

[12] U. Sander, P. Soukup, Design and operation of a pervaporation plant for ethanol dehydration, Journal of Membrane Science 36 (1988) 463–475. doi:https://doi.org/10.1016/0376-7388(88)80036-X.

[13] B. K. Srinivas, M. M. El-Halwagi, Optimal design of pervaporation systems for waste reduction, Computers & Chemical Engineering 17 (10) (1993) 957–970. doi:https://doi.org/10.1016/0098-1354(93)80077-Z.

[14] A. Dams, A. Fried, F. Hammann, Verfahren zur Gewinnung konzentrierter wäßriger Formaldehydlösungen durch Pervaporation. Patent DE4337231A1 (1993).

[15] H. Vandenmersch, T. Sirch, C. Hittinger, E. Danz, Verfahren zur Herstellung von alkoholischen Formaldehydlösungen mittels Membrantrennverfahren. Patent DE10004562A1 (feb 2000).

[16] N. Schmitz, C. F. Breitkreuz, E. Ströfer, J. Burger, H. Hasse, Separation of water from mixtures containing formaldehyde, water, methanol, methylal, and poly(oxymethylene) dimethyl ethers by pervaporation, Journal of Membrane Science 564 (2018) 806–812. doi:10.1016/j.memsci.2018.07.053.

[17] L. M. Vane, F. R. Alvarez, Effect of membrane and process characteristics on cost and energy usage for separating alcohol-water mixtures using a hybrid vapor stripping-vapor permeation process, Journal of Chemical Technology and Biotechnology 90 (8) (2015) 1380–1390. doi:10.1002/jctb.4695.

[18] C. Lipski, P. Coté, The use of pervaporation for the removal of organic contaminants from water, Environmental Progress 9 (4) (1990) 254–261. doi:10.1002/ep.670090420.

[19] H. Morishita, J. Masamoto, T. Hata, Process for producing high purity formaldehyde. Patent US4962235A (apr 1989).

[20] Sigma-Aldrich, Polyethylene glycol 400 data sheet (2020).
URL `https://pubchem.ncbi.nlm.nih.gov/substance/24852060`

[21] J. Masamoto, J. Ohtake, M. Kawamura, Process for producing formaldehyde and dervatives thereof. Patent US4967014 (feb 1989).

[22] M. Ott, H. H. Fischer, M. Maiwald, K. Albert, H. Hasse, Kinetics of oligomerization reactions in formaldehyde solutions: NMR experiments up to 373K and thermodynamically consistent model, Chemical Engineering and Processing: Process Intensification 44 (6) (2005) 653–660. doi:10.1016/j.cep.2003.07.004.

[23] N. Schmitz, E. Ströfer, J. Burger, H. Hasse, Conceptual Design of a Novel Process for the Production of Poly(oxymethylene) Dimethyl Ethers from Formaldehyde and Methanol, Industrial and Engineering Chemistry Research 56 (40) (2017) 11519–11530. doi:10.1021/acs.iecr.7b02314.

[24] C. Kuhnert, M. Albert, S. Breyer, I. Hahnenstein, H. Hasse, G. Maurer, Phase Equilibrium in Formaldehyde Containing Multicomponent Mixtures: Experimental Results for Fluid Phase Equilibria of (Formaldehyde + (Water or Methanol) + Methylal)) and (Formaldehyde + Water + Methanol + Methylal) and Comparison with Predictions, Industrial & Engineering Chemistry Research 45 (14) (2006) 5155–5164. doi:10.1021/ie060131u.

[25] Department of Chemical Engineering, Brigham University, Pravo, Utah, Thermophysical Properties Laboratory Project 801, Thermophysical Properties Laboratory Project 801 (2009).

[26] M. Albert, Thermodynamische Eigenschaften formaldehydhaltiger Mischungen, Phd thesis (1999).

[27] D. Bongartz, J. Burre, A. Mitsos, Production of Oxymethylene Dimethyl Ethers from Hydrogen and Carbon Dioxide - Part I: Modeling and Analysis for OME1, Industrial and Engineering Chemistry Research 58 (12) (2019) 4881–4889. doi:10.1021/acs.iecr.8b05576.

[28] N. Schmitz, Production of poly(oxymethylene) dimethyl ethers from formaldehyde and methanol, Phd thesis, Technical University of Kaiserslautern (2018).

[29] G. Towler, R. K. Sinnott, Chemical engineering design: principles, practice and economics of plant and process design, Elsevier, 2012.

[30] Chemical Engineering Plant Cost Index (2021).
URL `https://www.chemengonline.com/pci-home`

[31] Statista, Avg. Exchange Rate Euro/Dollar (2021).
URL `https://de.statista.com/statistik/daten/studie/200194/umfrage/wechselkurs-des-euro-gegenueber-dem-us-dollar-seit-2001/`

[32] Methanex, Methanex Monthly Average Regional Posted Contract Price History (2020).
URL `https://www.methanex.com/sites/default/files/MxAvgPrice Nov 30 2021.xls`

[33] Monitoringbericht 2018 (2018).
URL `Bundesnetzagentur Monitoringbericht 2018`

[34] R. Turton, Analysis, synthesis, and design of chemical processes, 3rd Edition, Prentice Hall PTR international series in the physical and chemical engineering sciences, Prentice Hall, Upper Saddle River, N.J, 2009.

[35] P. Stephan, S. Kabelac, M. Kind, D. Mewes, K. Schaber, T. Wetzel, VDI-Wärmeatlas: Fachlicher Träger VDI-Gesellschaft Verfahrenstechnik und Chemieingenieurwesen, Springer-Verlag Berlin Heidelberg, 2019.